Effect of Ce co-doping on KYF: Pr crystals

S. Veronesi, D. Parisi, F. Marchetti, M. Tonelli

Author's Accepted Manuscript

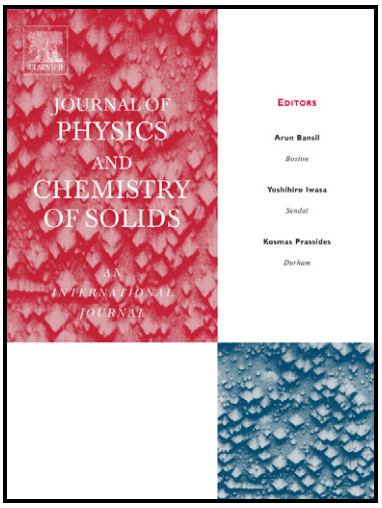

www.elsevier.com/locate/jpcs

Effect of Ce co-doping on KY_3F_{10}: Pr crystals

S. Veronesi, D. Parisi, F. Marchetti, M. Tonelli

PII: S0022-3697(10)00117-4
DOI: doi:10.1016/j.jpcs.2010.03.046
Reference: PCS 6155

To appear in: *Journal of Physics and Chemistry of Solids*

Received date: 28 July 2009
Revised date: 24 February 2010
Accepted date: 30 March 2010

Cite this article as: S. Veronesi, D. Parisi, F. Marchetti and M. Tonelli, Effect of Ce co-doping on KY_3F_{10}: Pr crystals, *Journal of Physics and Chemistry of Solids*, doi:10.1016/j.jpcs.2010.03.046

Effect of Ce co-doping on KY_3F_{10}:Pr crystals

S. Veronesi*,[a], D. Parisi[a], F. Marchetti[b], M. Tonelli[a]

[a] *NEST CNR-INFM and Dipartimento di Fisica, Università di Pisa, Largo B. Pontecorvo 3, I-56127 Pisa, Italy*
[b] *Dipartimento di Chimica e Chimica Industriale, Università di Pisa, Via Risorgimento 35, 56126 Pisa, Italy*

Abstract

A spectroscopic investigation on the effect of Ce^{3+} co-doping in fluoride KY_3F_{10}:Pr^{3+} crystals is presented. In particular spectroscopic measurements of three different samples of KY_3F_{10} crystal doped with 0.3at% Pr^{3+} and co-doped with 0at%, 0.17at% and 0.3at% Ce^{3+} are discussed. Details on the growth of the crystals are also reported. Measurements were performed in the temperature range 10 - 300 K. Fluorescence and lifetime measurements have shown a cross relaxation between $^3P_0$ - $^1D_2$ levels of Pr^{3+} and $^2F_{7/2}$ - $^2F_{5/2}$ of Ce^{3+}. Data exhibit that this effect is strictly related to the Cerium concentration.

Key words: Optical Materials, Crystal growth, Luminescence, Optical properties

PACS: 81.10.Fq, 42.70.Hj, 78.55.-m,

*Corresponding author. Tel.: +39 050 2214 184; fax: +39 050 2214 333.
Email address: veronesi@df.unipi.it (S. Veronesi)

1. Introduction

Fluoride crystals doped with trivalent rare earth (RE) ions are very important thanks to their large applications either as light source or as detectors. Solid state lasers based on trivalent RE in fact, emit in a wide wavelength range starting from mid IR to UV, with output power up to tens of watt [1, 2, 3]. Moreover good tunability and a great reliability are common characteristic of these lasers. The development of new visible solid state laser provides as well a spin-off for technology, as new generation of color displays. Fluoride single crystals are usually grown by different techniques, such as Bridgman, micro-pulling down and Czochralski. In literature are reported some papers regarding the growth of KY_3F_{10} as host material, doped with different RE, where it has been utilized or Bridgman [4] or micro-pulling down [5] or Czochralski [6] techniques. Fluoride single crystals which have a cubic symmetry, therefore optically isotropic, are attractive because they show the same refractive index independently on crystal orientation. This characteristic make them charming materials to develop cheap devices in ceramic form. For this reason we have investigated the luminescence of Pr^{3+} and Ce^{3+} in KY_3F_{10} host that is a face centered cubic compound with a structure similar to the fluorite (space group $Fm\bar{3}m$ [7]). Its crystal structure consists of two ionic groups $[KY_3F_8]^{2+}$ and $[KY_3F_{12}]^{2-}$ alternating along the three crystallographic directions. In the first group the fluorine atoms form an empty cube, while in the second one they form an empty cuboctahedron. The elementary cell contains 8 formula units and has a cell parameter a = 11.54 Å. The trivalent RE dopant substitute for the yttrium ions in sites of C_{4v} symmetry. KY_3F_{10} is easy to grow in large boules by Czochralski method, because it

melts congruently at a temperature about 1300K. Moreover it presents good optical and thermomechanical properties, all fascinating features for optically based applications [8]. Among RE dopant ions, Praseodymium shows quite strong visible emissions in the green, orange, red and infrared regions making it one of the most important dopant for laser applications [4, 5, 9, 10, 11]. In this paper we investigate the effect of Cerium co-doping on the green and red emission of KY_3F_{10}:Pr^{3+} crystal. Ce^{3+} has only one electron in the 4f orbital therefore it has only one excited energy level in the 4f configuration. The energy band gap of this level ($^2F_{7/2} \rightarrow {}^2F_{5/2}$) is about 3000 cm^{-1} that allows a phonon assisted energy transfer with the $^3P_0 \rightarrow {}^1D_2$ and $^3H_4 \rightarrow {}^3H_6$ levels of Pr^{3+} that are the starting and ending levels for the green and red lines [12, 13], making this co-doping of relevant interest. In Fig.1 we report a simplified energy levels scheme and the possible energy transfer processes of Pr^{3+} - Ce^{3+}.

2. Experimental set-up

Three KY_3F_{10} single crystals, doped with 0.3at% Pr^{3+} concentration and co-doped with 0at%, 0.17at% and 0.3at% Ce^{3+} concentration have been grown in a home-made Czochralski furnace from oriented seeds. The furnace is equipped with a conventional resistive heater and allow crystals growth up to 1400 K. The doping levels of RE, where reported, always refer to the concentration in the melt. The segregation coefficient for Pr^{3+} in KY_3F_{10} crystals is about 0.5 [12] in agreement with a measurement performed with an ICP-OES spectrometer on a sample of our Pr^{3+} doped crystal, with nominal dopant concentration in the melt of 0.3at%, which gave a value of 0.18at%.

Special care has been devoted to the quality of vacuum system, which has an ultimate pressure better than 10^{-7} mbar and the growth process was carried out in a high-purity (99.999%) argon atmosphere. Powders, from AC materials (Tarpon Springs, Fl., USA) had a 5N purity and the growth was performed starting from KY_3F_{10} as raw material and a proper amount of PrF_3 and CeF_3. The growth parameters were: temperature around 1328 K, pull rate 1 mm/h, rotation rate 5 RPM. As an example, in Fig.2 it is shown the boule doped with Pr^{3+} only, as grown. Moreover in order to confirm the single-crystal nature of our samples, we recorded x-rays backscattering Laue diffraction pattern of all samples. In order to verify the nature and the purity of phases present in the crystals used for this study, sections of each crystal have been hand milled in an agate mortar and their XRD patterns have been collected on a no-background sample holder. The powder diffraction patterns have been carried out in the 2θ range 10-90° by steps of 0.02° using a Philips PW1050/25 Bragg-Brentano diffractometer. The measurements have been performed at room temperature using a Cu source with accelerating voltage 40 kV, tube current 20 mA and a graphite monochromator on the secondary beam ($K\alpha$, $\lambda = 1.54184$ Å). The diffracted beam has been detected using a scintillation counter integrating for 10 s/step.

Our spectroscopic experimental setup allows both static and dynamic measurements, to determine absorption spectra at room temperature and fluorescence spectra and levels lifetime from 10 K up to room temperature.

The measurement of the absorption coefficients have been performed by means of a VARIAN CARY 500 Scan spectrophotometer operating in the range 180-3200 nm. Absorption spectra have been recorded in the region

190-750 nm in order to check the absorption bands relatives to both Ce^{3+} and Pr^{3+}. A special care was reserved to the region 430-490 nm, with a resolution of 0.15 nm, because of the small bandwidth of Pr^{3+} lines and in order to chose the best excitation wavelength.

The fluorescence measurements have been performed by exciting the samples with a Nichia GaN NDB7112E blue laser diode tuned at 446 nm, according to the absorption spectrum of KY_3F_{10}:Pr^{3+}. The samples were placed inside a CTI CRYOGENICS helium cryo-cooler which allows measurements in the range 10-300 K. The laser beam was focused onto the sample by means of a 10 cm focal length lens. The fluorescence was collected by a 7.5 cm focal length infrasil lens, perpendicularly with respect to the excitation beam in order to minimize pump spurious scattering collection. Luminescence was focused on the entrance slit of a 32 cm focal length Jobin-Yvon monochromator and opportunely filtered (λ_t = 460 nm). The monochromator was equipped with three (1200, 600, 300 gr/mm) diffraction gratings to operate in the range 300-3000 nm. Signal was detected by a R1464 Hamamatsu photomultiplier and acquired by a SR830 Lock-in Amplifier. The resolution of the fluorescence spectra was 0.13 nm in the range 450-750 nm. The acquired spectra were normalized for the optical response of the system using a blackbody source at 3000 K. Levels lifetime were measured by means of a pulsed tunable Ti:Al_2O_3 laser with a 10 Hz repetition rate and 30 ns pulse width doubled by a BBO crystal. In all lifetime measurements the pulse energy was reduced as much as possible to minimize power dependent effects. To reduce an artificial lifetime lengthening due to radiation trapping, laser beam was focused near the edge of the crystal utilized for light collection. To prevent

the detection of scattered laser light, the collected radiation was suitably filtered. Signal was detected by a R1464 Hamamatsu photomultiplier and amplified, with an overall response time of about 1 μs. Data acquisition was performed with a digital oscilloscope connected to a computer.

3. Experimental results

X-ray characterization

XRD diffractograms as a function of Pr^{3+} and Ce^{3+} concentration are shown in Fig.3. The patterns of our samples (B, C, D) are compared with the pattern A, calculated [14] from the known structure of KY_3F_{10} [7]. The exact agreement in line positions suggests the doped samples maintain the crystal structure of pure KY_3F_{10} and no different phases are present. The differences in line intensities may be ascribed to preferential orientation effects.

Absorption measurements

The absorption measurements have been performed at room temperature with non polarized light, due to crystal isotropy. Spectra have been recorded in the range 430-490 nm to determine the Pr^{3+} absorption lines and in the range 190-350 nm to determine the Ce^{3+} absorption lines and to check doping levels. The results obtained for all the samples are shown in Fig.4. Pr^{3+} peaks can be assigned to the $^3P_0$, $^3P_1$ + $^1I_6$ and $^3P_2$ manifolds and they exhibit the maximum absorption at 446 nm with an α coefficient of 0.9 cm^{-1}. As it is possible to see in Fig.4, the 480 nm line assigned to $^3P_0$ singlet, present a small secondary peak (486 nm) that is not present in other hosts like $LiLuF_4$

[15]. Probably this effect is due to the peculiarity of KY_3F_{10} crystal structure that is slightly disordered, as previously discussed. The transition of the Ce^{3+} derives from the $^2D_{5/2}$ and $^2D_{3/2}$ manifolds.

Fluorescence and lifetime measurements

As a preliminary investigation we performed the fluorescence spectra, for all the samples, at room temperature in the range 465-750 nm in order to determine which bands were mainly affected by the Ce^{3+} presence. In Fig.5a is reported the the whole fluorescence spectrum together with transition assignment. It is possible to observe in Fig.5, that the Ce^{3+} effect is restricted to the transitions in the range 590-608 nm. In the particular of Fig.5b our samples (0at%, 0.17at% and 0.3at% Ce^{3+} respectively) are compared. We want underline that the emission lines mainly affected by the Ce^{3+} presence, belong to $^1D_2 \rightarrow {}^3H_4$ and $^3P_0 \rightarrow {}^3H_6$ transitions. These two bands are quite close and at room temperature they are appreciably mixed. For this reason, focusing our attention on this wavelength region, we perform fluorescence and decay time measurements at low temperature where the spectral lines are more resolved and the mixing is strongly reduced.

Fluorescence spectra has been recorded at 10, 50 and 77 K. Measurements performed at 10 K for all the samples are shown in Fig.6a. From this figure it is evident that the contribution of $^1D_2$ and $^3P_0$ is resolved. The main comb, around 610 nm, comes from the transition $^3P_0 \rightarrow {}^3H_6$. The Ce^{3+} co-doping produces a phonon assisted energy transfer as previously discussed and this effect increases with increasing Ce^{3+} concentration. In fact in Fig.6a it is well underlined the decrease in the 606 nm line fluorescence intensity ($^3P_0 \rightarrow {}^3H_6$) and the contemporary enhancement of the 601 nm line ($^1D_2 \rightarrow {}^3H_4$). More-

over in Fig.6b it is shown the intensity of the 601 nm line as a function of both temperature and Ce^{3+} doping level. As it is evident from the figure, intensity increases with the Ce^{3+} concentration and decreases as temperature rises up to room temperature.

For a further deepening, the dynamic behavior of the two manifolds $^3P_0$ and $^1D_2$ as a function of temperature was investigated. Lifetime measurements had been performed, for all the samples, at 10, 50 and 77 K. Moreover we perform two set of lifetime measurements: the first one to check the decay time of $^3P_0$ only, observing at 645 nm where $^1D_2$ manifold has no emission lines; the second one to monitor the affected mix transitions $^3P_0$ and $^1D_2$, observing at 606 and 601 nm. The decay time of $^3P_0$ manifold, observing at 645 nm, results to be independent from Ce^{3+} doping level and from temperature within the measurements errors. From data analysis it is possible to obtain a single exponential behavior with a lifetime $\tau = 39 \pm 2$ μs. This result is in agreement with that shown in literature [12, 15].

The second set of measurements was performed with a resolution of about 1.3 nm, in order to avoid the superpositions of close transitions $^3P_0$ and $^1D_2$. In Tab.1 are reported the values for decay times of this set of measurements together with the statistical fitting errors. Analyzing the line at 606 nm, it is possible to observe that the sample without Ce^{3+} shows a lifetime equal to the $^3P_0$ manifold with a single exponential decay curve (see Fig.7c). The second sample, corresponding to a Ce^{3+} concentration of 0.17at%, presents a lifetime value slightly increased, preserving however a single exponential behavior within the fit error. The longer lifetime measured it is presumably due to a very low mixing with $^1D_2$ level which the fitting analysis cannot

discriminate, but it is seen as a longer lifetime of $^3P_0$. In fact it is possible to observe a slightly deviation of data points from fitting curve. The third sample, corresponding to a Ce^{3+} concentration of 0.3at%, presents a decay curve that is describable with a double exponential behavior as shown in Fig.7a. The analysis gives a first fast decay time compatible with a $^3P_0$ lifetime and a longer value that we attribute to the $^1D_2$ manifold. In fact only $^3P_0$ and $^1D_2$ manifolds have transitions in this wavelength region and we expect a longer lifetime for $^1D_2$ manifold due to its lower energy and to spin selection rule as reported in detail in [16]. The particular in Fig.7b shows the increase of the signal at the beginning of the decay curve due to the cross relaxation mechanism.

Analyzing the line at 601 nm it is possible to observe that the sample without Ce^{3+} shows a double exponential decay behavior due to the superposition of the decay from $^3P_0$ and $^1D_2$ manifolds, each with its proper decay time. The measured lifetime values are in agreement with those obtained for the third sample at 606 nm just discussed, pointing out an appreciable line mixing. Both samples doped with Ce^{3+} show a single exponential behavior with a lifetime $\tau = 280 \pm 5$ μs which is in agreement with the $^1D_2$ manifold lifetime reported in literature [13].

In our opinion this behavior underline that the effect of co-doping Pr^{3+}-Ce^{3+} is to increase cross relaxation $^3P_0 \rightarrow {}^1D_2$, $^3H_4 \rightarrow {}^3H_6$ pushing the 601 nm level lifetime toward a pure $^1D_2$ transition (see Fig.1). In fact, as it is possible to see in Fig.1 there is a good matching between the $^2F_{7/2} \rightarrow {}^2F_{5/2}$ transition energy (about 3000 cm^{-1}) of Ce^{3+} and $^3P_0 \rightarrow {}^1D_2$, $^3H_4 \rightarrow {}^3H_6$ of Pr^{3+} (about 3800 cm^{-1}) [17]. Such a small energy difference can be easily bridged with

the help of few phonons. Moreover at the highest Ce^{3+} concentration this effect become important even on the 606 nm line, that is a pure $^3P_0$ decay in all the sample but the heavier co-doped, where there is an appreciable line mixing. The values obtained for the $^1D_2$ lifetime agree with those obtained in ref [13] where a Pr^{3+} doping level in the crystal slightly less than our is utilized. We observe on the contrary a much shorter $^1D_2$ decay time reported in ref [16] probably due to an higher Pr^{3+} concentration (more than a factor 2) which enhances cross-relaxation amount.

4. Conclusion

We have observed the effect of Ce^{3+} co-doping on fluoride KY_3F_{10} crystals doped with Pr^{3+}. In particular manifolds around 601 and 606 nm are affected by the Ce^{3+} presence because of a phonon assisted energy transfer process between $^3P_0$ - $^1D_2$ of Pr^{3+} and $^2F_{7/2}$ - $^2F_{5/2}$ of Ce^{3+}. We report the growth of three mono-crystals and absorption, fluorescence and lifetime measurements of three samples: KY_3F_{10}: 0.3at% Pr^{3+}-0at% Ce^{3+}, KY_3F_{10}: 0.3at% Pr^{3+}-0.17at% Ce^{3+} and KY_3F_{10}: 0.3at% Pr^{3+}-0.3at% Ce^{3+}. Fluorescence and lifetime measurements were performed in the temperature range 10 - 300 K while absorption spectra were recorded at room temperature. The most important effect is the decrease of the 606 nm level fluorescence with the increase of Ce^{3+} concentration and the contemporary increase of 601 nm level fluorescence. The effect extent is also temperature dependent. The detailed analysis of the lifetimes of these levels shows a mixing of the $^3P_0$ - $^3H_6$ and $^1D_2$ - $^3H_4$ transitions more and more evident increasing the Ce^{3+} concentration. Since the value of the energy levels difference between $^2F_{7/2}$ - $^2F_{5/2}$ of Ce^{3+}

allows a phonon assisted energy transfer with the manifolds $^3P_0$ - $^1D_2$ of Pr^{3+}, meaning a significant increase of the $^1D_2$ manifold population. In future, optimizing the doping level of Cerium with respect to Praseodimium, it will be possible to obtain a more efficient population of $^1D_2$ manifold.

5. Acknowledgements

Authors wish to thank I. Grassini, for preparing the samples, Dr. F. Cornacchia for helpful discussions and H.P. Jenssen and A. Cassanho for their invaluable aid in crystal growth.

References

[1] A. Dergachev, K. Wall, and P.F. Moulton, "A CW Side-Pumped Tm:YLF Laser" Advanced Solid State Laser **68**, (2002), 343.

[2] K.S. Lai, W.J. Xie, R.F. Wu, Y.L. Lim, E.Lau, L. Chia, and P.B. Phua, "A 150W 2-micron diode-pumped Tm:YAG laser" Advanced Solid State Laser **68**, (2002), 535.

[3] D. Alderighi, G. Toci, M. Vannini, D. Parisi, S. Bigotta, and M. Tonelli, "High efficiency UV solid state lasers based on Ce:$LiCaAlF_6$ crystals" Appl. Phys. B **83 n. 1**, (2006), 51-54.

[4] P. Camy, J. L. Doualan, R. Moncorgé, J. Bengoechea, and U. Weichmann, "Diode-pumped Pr^{3+}:KY_3F_{10} red laser," Opt. Lett. **32**, (2007) 1462-1464.

[5] K.J. Kim, A. Jouini, A. Yoshikawa, R. Simura, G. Boulon, T. Fukuda, "Growth and optical properties of Pr,Yb-codoped KY_3F_{10} fluoride single crystals for up-conversion visible luminescence" J. Crystal Growth **299**, (2007) 171-177.

[6] A. Rapaport, J. Milliez, F. Szipöcs, M. Bass, A. Cassanho and H. Jenssen, "Properties of a new, efficient, blue-emitting material for applications in upconversion displays: Yb,Tm:KY_3F_{10}" Appl. Opt. **43**, (2004) 6477.

[7] A. Grzechnik, J. Nuss, K. Friese, J.-Y. Gesland and M. Jansen, "Refinement of the crystal structure of potassium triyttrium decafluoride,KY_3F_{10}" Z. Kristallogr. NCS **217**, (2002) 460.

[8] K. Friese, H. Kruger, V. Kahlenberg, T. Balic-Zunic, H. Emerich, J-Y. Gesland and A. Grzechnik, "Study of the temperature dependence of the structure of KY_3F_{10}" J. Phys.: Condens. Matter **18**, (2006), 2677-2687.

[9] F. Cornacchia, A. Di Lieto, M. Tonelli, A. Richter, E. Heumann, and G. Huber, "Efficient visible laser emission of GaN laser diode pumped Pr-doped fluoride scheelite crystals," Opt. Express **16**, (2008) 15932-15941.

[10] A. Richter, E. Heumann, E. Osiac, G. Huber, W. Seelert, and A. Diening, "Diode pumping of a continuous wave Pr^{3+} doped $LiYF_4$ laser," Opt. Lett. **29**, (2004) 2638-2640.

[11] A. Richter, E. Heumann, G. Huber, V. Ostroumov, and W. Seelert, "Power scaling of semiconductor laser pumped Praseodymium-lasers," Opt. Express **15**, (2007) 5172-5178.

[12] A. Richter, "Laser parameters and performance of Pr^{3+}-doped fluorides operating in the visible spectral region", Amburg University PhD Thesis (2008).

[13] J-P R Wells, M. Yamaga, T.P.J. Han and H.G. Gallagher, "Infrared absorption, laser excitation and crystal-field analyses of the C_{4v} symmetry centre in KY_3F_{10} doped with Pr^{3+}", J. Phys.; Condens. Matter **12** (2000) 5297-5306.

[14] W. Kraus, G. Nolze, "PowderCell", rel. 2.3, Federal Institute for Materials Research and Testing, Berlin, Germany, (1999).

[15] F. Cornacchia, A. Richter, E. Heumann, G. Huber, D. Parisi and M. Tonelli, "Visible laser emission of solid state pumped $LiLuF_4$: Pr^{3+}", Optics Express **15 n. 3,** (2007) 992-997.

[16] M. Laroche, A. Braud, S. Girard, J.L Doualan, R. Moncorgé, M. Thuau and L.D. Merkle, "Spectroscopic investigations of the 4f5d energy levels of Pr^{3+} in fluoride crystals by excited-state absorption and two-step excitation measurement" J. Opt. Soc. Am. B, **16 n.12,** (1999) 2269-2277.

[17] E. Sani, A. Toncelli, and M. Tonelli, "Effect of Cerium codoping on Er:BaY_2F_8 crystals," Opt. Express **13**, (2005) 8980-8992.

6. Figure Caption

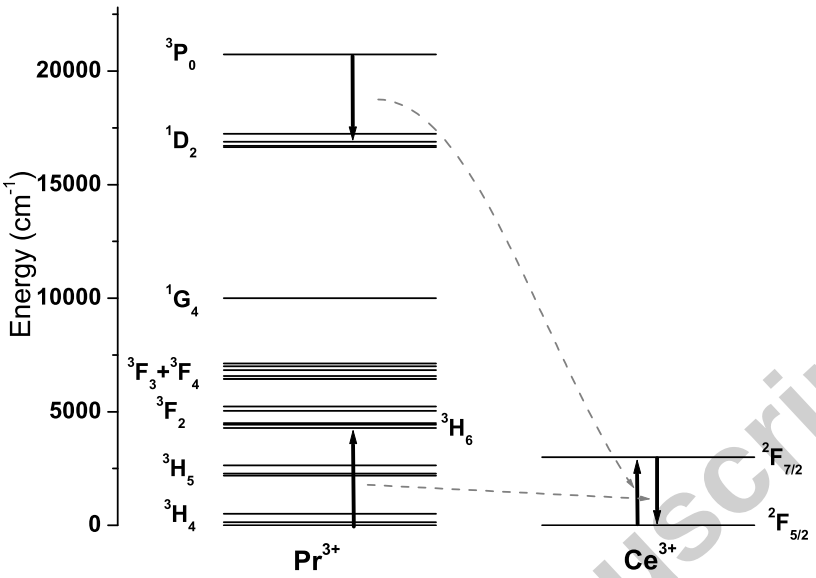

Figure 1: Energy levels of Pr^{3+}-Ce^{3+} in KY_3F_{10}

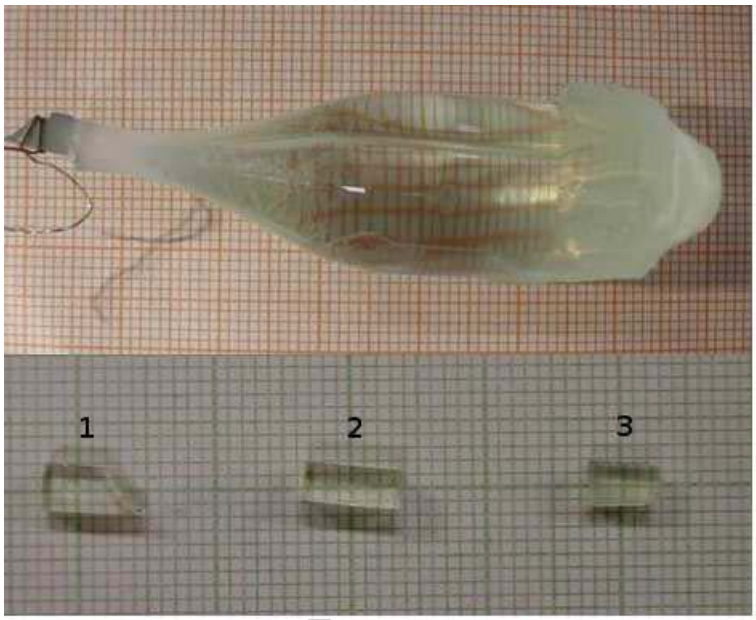

Figure 2: Pictures of the KY_3F_{10}:Pr as grown (boule dimensions about 60 mm length and 20 mm diameter) and the three polished samples used for spectroscopic investigations. 1)KY_3F_{10}:0.3at%Pr; 2)KY_3F_{10}:0.3at%Pr-0.17at%Ce; 3)KY_3F_{10}:0.3at%Pr-0.3at%Ce. All the backgrounds are in millimeter paper.

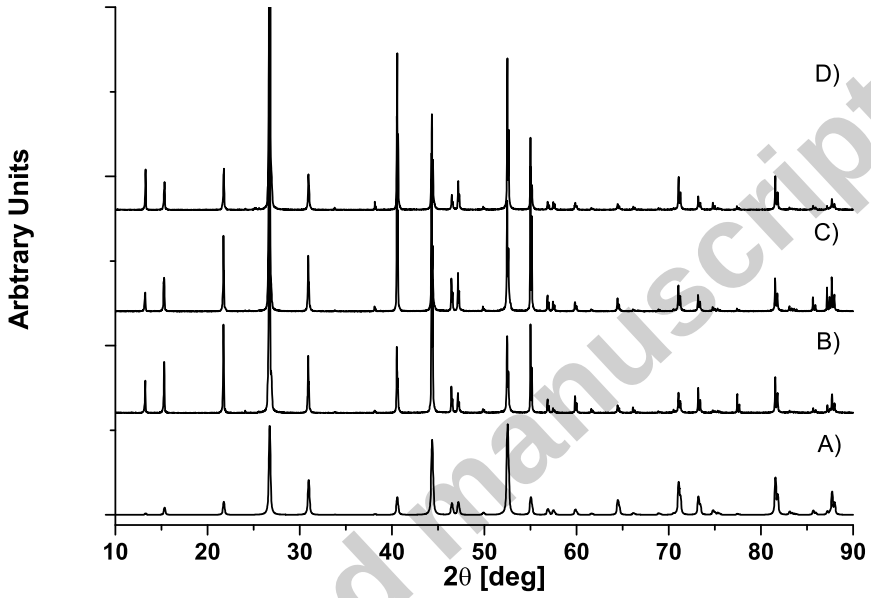

Figure 3: X-ray diffraction patterns of the undoped (calculated) (A) and 0.3% Pr, x% Ce:KY_3F_{10} single crystals [x = 0at% (B), x = 0.17at% (C), x = 0.3at% (D)].

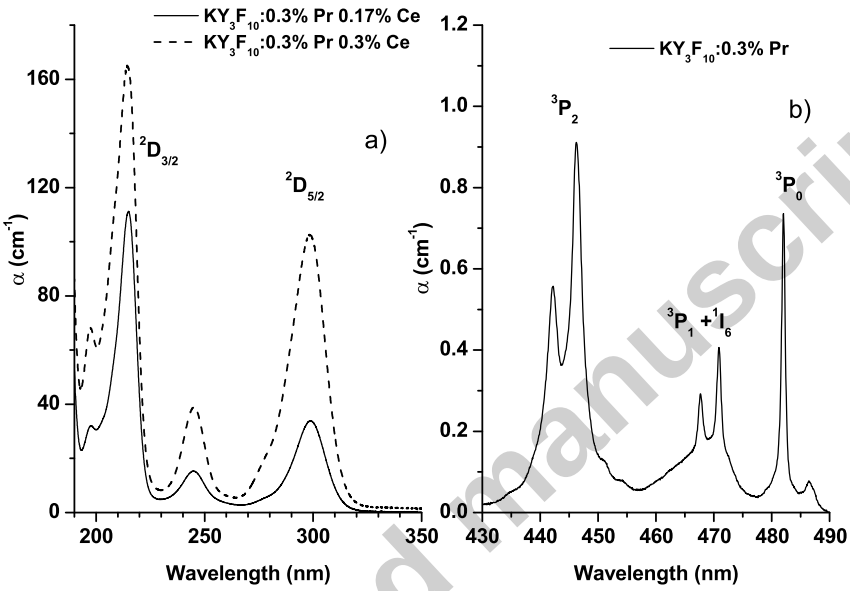

Figure 4: Absorption spectra of KY_3F_{10} samples: a) UV bands of 0.17% and 0.3% Ce^{3+}; b) blue band of Pr^{3+}

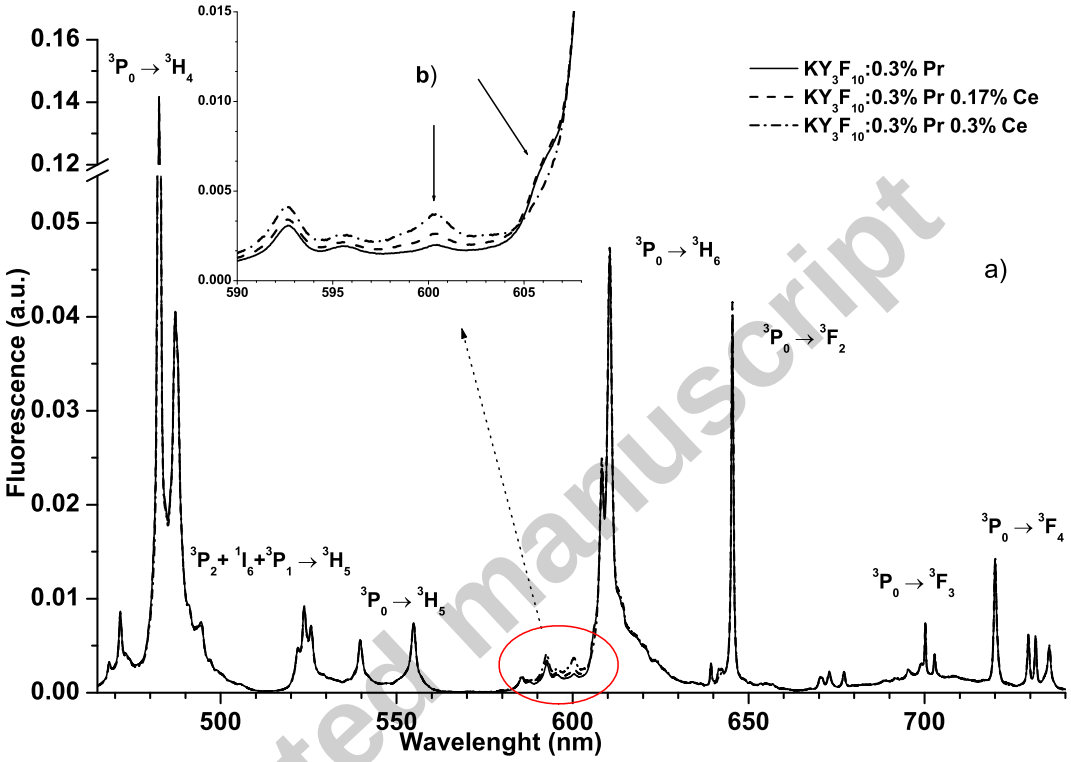

Figure 5: Room temperature fluorescence spectra of KY_3F_{10} samples: a)whole spectrum for all the sample from 465 to 750 nm; b)particular from 590 to 608 nm as a function of Cerium concentration

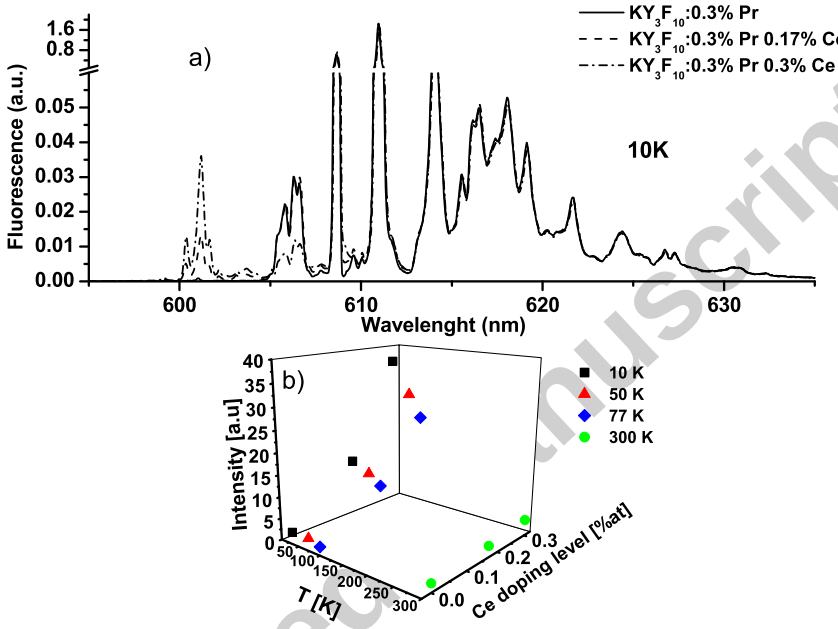

Figure 6: a) Fluorescence spectra at 10 K in the range 595-635 nm of KY_3F_{10} samples; b) intensity of the line at 601 nm as a function of temperature and Ce^{3+} doping level

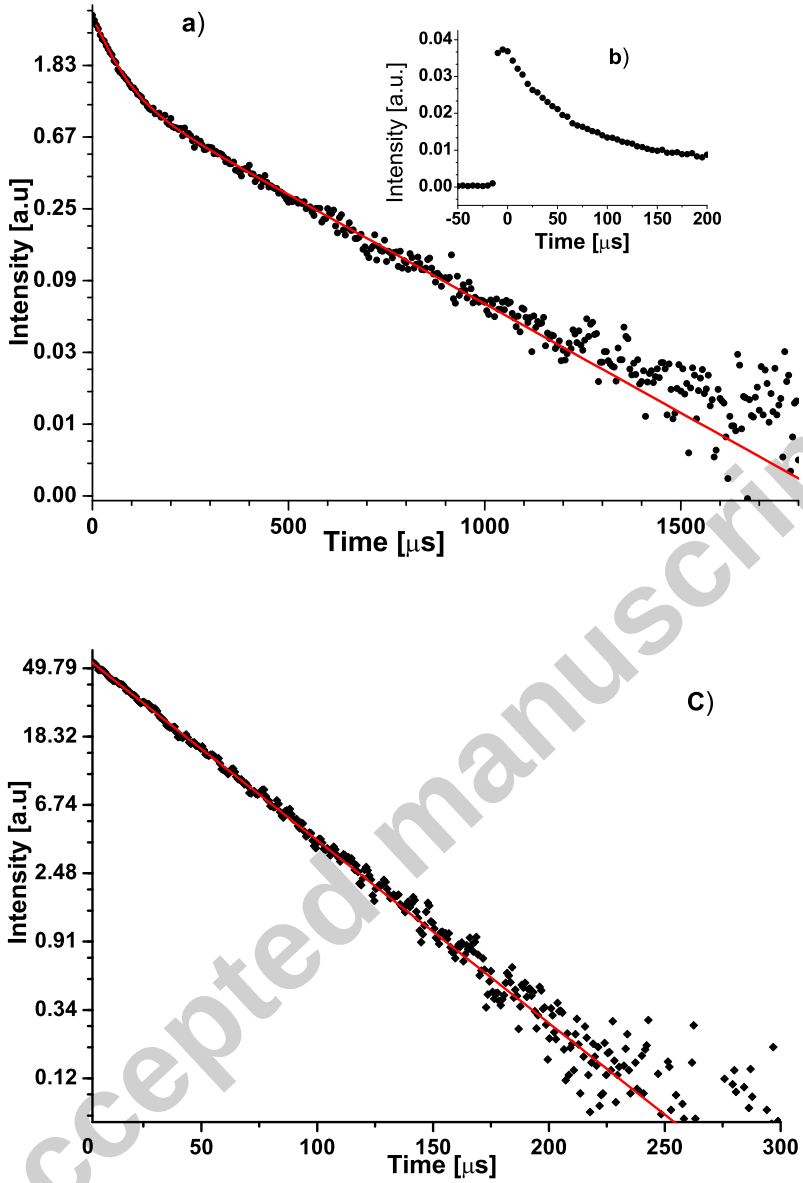

Figure 7: Decay time curve at 50 K observed at the wavelength of 606 nm for: KY_3F_{10}:0.3%Pr-0.3at% Ce (a and b), KY_3F_{10}:0.3%Pr (c) samples. a)Double exponential fitting; b)A particular of the beginning of the decay curve; c) Single exponential fitting.

Table 1: Second set of decay time measurements (resolution 1.3 nm).

Crystal	T[K]	$\tau(\mu s)$			
		λ_2(606 nm)		λ_3(601 nm)	
		$^3P_0$	$^1D_2$	$^3P_0$	$^1D_2$
KY_3F_{10}:0.3%Pr	10	37.3 (0.2)	-	49 (4)	316 (40)
	50	42.5 (0.5)	-	48 (8)	314 (50)
	77	41.8 (0.2)	-	46 (5)	294 (45)
KY_3F_{10}:0.3%Pr0.17%Ce	10	46.2 (0.5)	-	-	297 (1)
	50	46.3 (0.5)	-	-	295 (1)
	77	44.5 (0.2)	-	-	288 (2)
KY_3F_{10}:0.3%Pr0.3%Ce	10	43 (2)	273 (16)	-	262 (2)
	50	42.6 (1.2)	266 (15)	-	264 (3)
	77	42.2 (0.9)	299 (53)	-	262 (1)